*Chaotic Modeling and Simulation (CMSIM)* **2: 197-206, 2016**

# The Complete Bifurcation Analysis of Switching Power Converters with Switching Delays

Dmitrijs Pikulins[1]

[1] Institute of Radioelectronics, Riga Technical University, Riga, Latvia
(E-mail: dmitrijs.pikulins@rtu.lv)

**Abstract.** The nonlinear dynamics of switching power converters has been actively studied during several last decades, proving the existence of extremely complex dynamical scenarios and uncommon routes to chaos in this kind of circuits. The main assumption in the majority of researches was that the control circuitry consisted of ideal elements, discarding all parasitics of feedback circuitry components. However, recently it has been shown that the inherently arising nonidealities, such as delays, could lead to the drastic changes in the overall dynamics of the system. This research is dedicated to the investigation of the effects of the delays on the global nonlinear behavior of switching DC-DC converters on the basis of complete bifurcation analysis, providing the most comprehensive information on the causes and consequences of all nonlinear phenomena in the systems under study.
**Keywords:** Bifurcations, chaos, non-smooth phenomena, switching power converters

## Introduction

Active research performed during several last decades showed that the commonly used linearized models, describing the dynamics of switching power converters (SPC) are not capable of predicting the majority of instabilities, occurring in those systems [1,2]. Thus the classical models fail to provide reliable information for the feedback designers that would allow the development of stable control loops. The limited applicability of mentioned models has led to the development of some alternative approaches, based on non-linear models and analysis methodologies. While making the study of global dynamics of these systems more complicated, the latter approaches allow increasing the robustness and reliability of designed systems as the great amount of new unstable and potentially dangerous regimes could be detected.

The vast majority of researchers, working on the analysis of non-linear dynamics of SPC, have focused on the development of simplified models that could be used within their investigations. However, it has been shown that ignoring some unavoidable non-idealities of the control circuitry may lead to erroneous results and misinterpretation of analytically obtained data [3]. One of the most noticeable effects, that should be taken into account during the analysis

Received: 28 March 2015 / Accepted: 27 December 2015

ISSN 2241-0503

of such feedback controlled systems, is the inherent delay of each component of the control loop. The delay of individual element in the analog feedback loop is not large enough to influence the global dynamics of the system. Though as all the delays are summed together, the time lag in the propagation of the control signal becomes essential.

The current paper studies the effects of the magnitude of the overall delay on the dynamics of one of the most widely used SPC – boost converter under current-mode control. It is assumed that the analog feedback loop is implemented and the appropriate values of delays are introduced. The analysis of bifurcation patterns is based on the discrete-time model of mentioned DC-DC converter and the Method of Complete Bifurcation Groups (MCBG).

The structure of the paper is as follows. Second section describes the principles of operation of the boost converter as well as presents the corresponding model. Third section provides the complete bifurcation analysis of SPC, changing the most relevant circuit parameters. The last section is dedicated to conclusions about the results obtained in Section 3, defining some common points and showing the perspective of future research.

## 2 Model of the boost converter with delays

The simplified schematic of the boost type SPC under current-mode control including delay is shown in the Fig.1. It consists of two active elements: capacitor *C* and inductor *L*; two switching elements: one of them marked as *S* could be a MOSFET transistor (the state of which is controlled by the voltage applied to the gate), the second one – *D*–is the diode (that is turned *ON* or *OFF* in accordance to the difference of voltages between its terminals). *R*, $V_{in}$ and $V_{out}$ represent accordingly simple resistive load, input and output voltages. $\Delta t_d$ represents the total delay of all elements in the control loop.

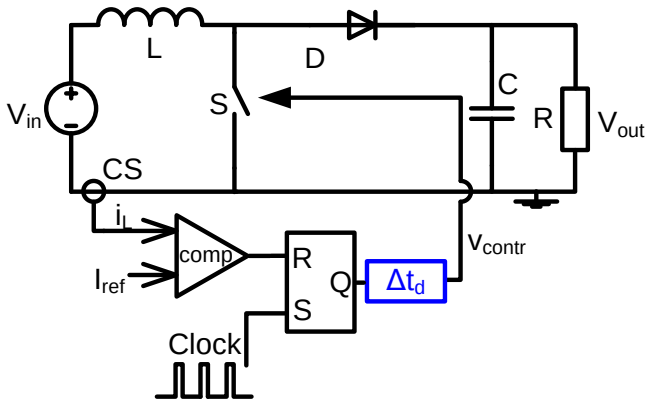


Fig.1. Simplified schematics of boost SPC under current-mode control

The control circuitry, shown above the main power plant, consists of current sensor (CS), comparator (comp), RS type flip-flop as well as clock element.

The principle of operation is as follows. When the switch *S* is in the *ON* (conducting) state, the energy is transferred to the inductor and the load is provided with the necessary amount of energy by the output capacitor. During the *OFF* interval the required output voltage is maintained by the input voltage and the energy released from the collapsing magnetic field of the inductor.

As it could be seen from Fig.1, the position of the switching element *S* is defined by the output signal of the control circuitry $v_{contr}$. In the case of ideal control loop with $\Delta t_d=0$, the switch is turned *ON* at the arrival of the next clock pulse and is switched *OFF* as the value of inductor current, obtained from the current sensor, reaches the reference value (see Fig. 2.a). However, real analog control loops include the non-zero delay, which is formed by the sum of current sensors', comparator', RS flip-flops' as well as MOSFET drivers' switching delays that are unified in the single block $\Delta t_d$ in the Fig.1.

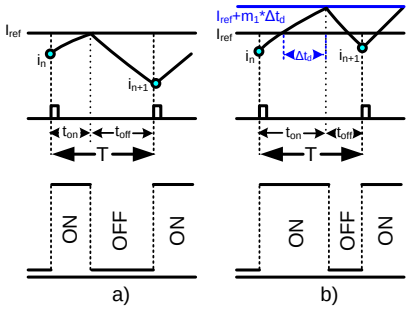


**Fig.2. Waveforms of the inductor current and control signals: a) ideal case; b) including delay $\Delta t_d$**

The delay causes the switch not to turn *OFF* at the moment the control parameter reaches some reference value defining new dynamical scenarios (see Fig. 2.b). The maximal value of sensed inductor current in this case is not limited by predefined reference $I_{ref}$ and becomes dependent on the delay, reaching the value $I_{ref}+m_1*\Delta t_d$, where the slope of the rising inductor current $m_1=V_{in}/L$.

The dynamics of this type of energy converters could be described by systems of differential equations. However, the bifurcational analysis on the basis of this model would require great amount of computations. Another more effective approach is the use of discrete-time model in the form of iterative map that would allow obtaining exact values of inductor current and capacitor voltage samples at every switching instant without excessive effort [4]. The proposed

model for the boost converter including the delay is as follows.

First, it should be noted that the overall dynamics of the converter is governed by the positions of the samples of inductor current in correspondence to the two borderlines shown in Fig.3. The first borderline defines the case when the inductor current reaches the shifted reference value exactly at the arrival of next clock pulse (see Fig. 3.a). The second borderline represents $i_n$ value for which the next sample $i_{n+1}$ falls exactly to the $I_{ref}$ for the falling inductor current (see Fig. 3.b).

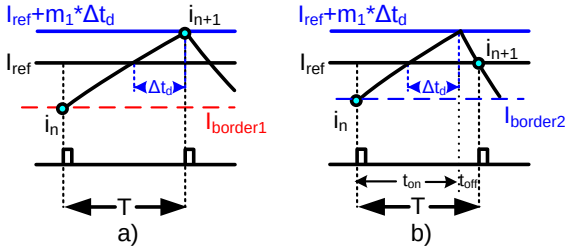


**Fig. 3. Definition of borderlines and corresponding positions of inductor current samples: a) $I_{border1}$; b) $I_{border2}$**

Thus the borderlines are:

$$I_{border1} = I_{ref} + m_1(\Delta t_d - T)\,, \tag{1}$$

$$I_{border2} = I_{border1} + m_1 \Delta t_d / \alpha\,, \tag{2}$$

where $m_1 = V_{in}/L$, $\Delta t_d$ - the value of delay, $T$– switching period, $I_{ref}$– reference current, $L$ - value of inductance, $R$– load resistance; parameter $\alpha$ could be found using methodology proposed in [5] as the positive solution of this quadratic equation:

$$(1+\alpha)^2 V_{in}/R + \alpha V_{in} T/3L = I_{ref} + m_1 \Delta t_d\,. \tag{3}$$

Thus, taking into account (1)-(3), the discrete-time model is defined as:

1. if $i_n < I_{border1}$:

$$v_{n+1} = v_n \exp(-T/RC)$$
$$i_{n+1} = i_n + V_{in} T/L\,; \tag{4}$$

2. if $I_{border1} < i_n < I_{ref}$:

$$v_{n+1} = \exp(-mt_{off})\left[K_1 \cos(\mu t_{off}) + K_2 \sin(\mu t_{off})\right] + V_{in} \tag{5}$$

$$i_{n+1} = \exp(-mt_{off})\begin{bmatrix}(K_1\cos(\mu t_{off}) + K_2\sin(\mu t_{off}))(1/R - mC) + \\ + \mu C(-K_1\sin(\mu t_{off}) + K_2\cos(\mu t_{off}))\end{bmatrix} + V_{in}/R\ ;$$

3. if $I_{ref}<i_n<I_{ref}+m_1\Delta t_d$, then there are two possible scenarios, which are dependent on the value of the inductor current in the previous cycle:

3.1. if $I_{border1}<i_{n-1}<I_{border2}$, than the dynamics of the system between $i_n$ and $i_{n+1}$ is governed by:

$$\begin{aligned} v_{n+1} &= \exp(-mT)\left[K_3\cos(\mu T) + K_4\sin(\mu T)\right] + V_{in} \\ i_{n+1} &= \exp(-mT)\begin{bmatrix}(K_3\cos(\mu T) + K_4\sin(\mu T))(1/R - mC) + \\ + \mu C(-K_3\sin(\mu T) + K_4\cos(\mu T))\end{bmatrix} + V_{in}/R\ ; \end{aligned} \quad (6)$$

3.2. if $i_{n-1}<I_{border1}$,than the dynamics of the system is governed by (5),

where: $p = 1/\sqrt{LC}$ ; $\mu = \sqrt{p^2 - m^2}$ ; $K_1 = v_n\exp(-2mt_{on}) - V_{in}$ ;

$K_2 = \left((I_{ref} + m_1\Delta t_d)/C - m(v_n\exp(-2mt_{on}) + V_{in})\right)/\mu$ ; $K_3 = v_n - V_{in}$ ;

$K_4 = \left(i_n/C - m(v_n + V_{in})\right)/\mu$ ; $t_{on} = (I_{ref} - i_n)/m_1 + \Delta t_d$ , $t_{off} = T - t_{on}$ ;

$m_1 = V_{in}/L$ .

Parameters of the system under investigation are as follows: $V_{in}$=3.3 (V); $L$=150 (μH); $C$=2 (μF); $R$=40 (Ω); $I_{ref}$= 0.2…0.7 (A); T=10 (μs); $\Delta t_d$=(0…0.2)*$T$ (s).

## 3 Complete bifurcation analysis

The analysis of bifurcation patterns in this paper is based on the relatively new methodology – Method of Complete Bifurcation Groups – originally developed in the Institute of Mechanics of Riga Technical University for the analysis of complex dynamics of highly nonlinear mechanical systems [6]. This approach has been applied to the great variety of dynamical systems, including mechanical, biological and electrical ones [7-9]. The main distinctive feature of the MCBG is that the construction of bifurcation diagrams is not based on the widely used brute-force approach, when only stable periodic regimes are plotted using the process of simple iterations (also called natural transition). The mentioned brute-force method does not provide the complete information even about all existing stable regimes, not to mention unstable ones that are not taken into account in this approach. The MCBG is based on the numerical calculation of all stable and unstable periodic regimes (up to period of interest) in the system with following continuation of branches in the bifurcation diagram as some of the system's parameters are varied. This approach allows the construction of complete bifurcation diagrams, depicting even small regions of periodicity as well as unfolding unambiguous interconnections between different periodic as well as chaotic modes of operation.

On the basis of MCBG the complete bifurcation diagrams for the boost type converters with ideal feedback loop and for the system taking into account the delays in the control circuitry, have been constructed. The most obvious choice of the primary bifurcation parameter is the value of $I_{ref}$ that could be changed during the operation of the SPC in order to preserve the desired output voltage.

The complete bifurcation diagrams obtained for the system with a various delays allow detection of some most distinctive changes in nonlinear dynamics of DC-DC converters as we vary the bifurcation parameter.

First, the complete bifurcation diagram for $\Delta t_d$=0 (i.e. in the ideal model without any delays) is constructed (see Fig. 4). Dark lines represent stable periodic regimes, light lines – numerically calculated unstable regimes, dashed lines depict the borderlines defined in (1) and (2), the shaded area represents the chaotic mode of operation.

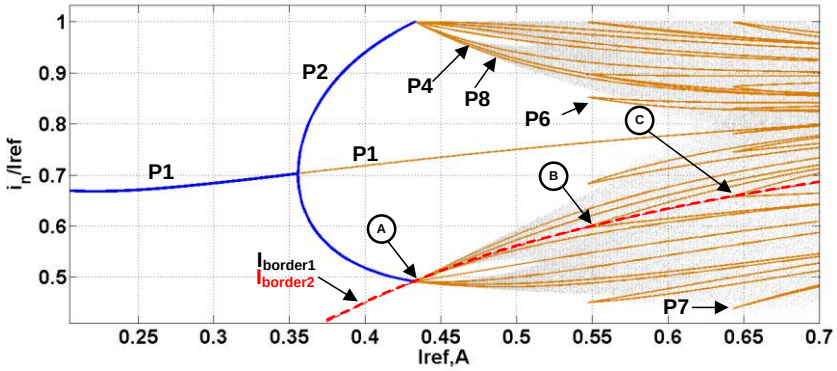


**Fig.4. Complete bifurcation diagram of the boost converter with ideal control loop**

The increment of reference current leads to the smooth transition from *P1* to *P2* operation through classical period-doubling bifurcation at $I_{ref}$≈0.36 (A). At point *(A)* the border collision (BC) with $I_{border1}$ and $I_{border2}$ appears (these borders overlap in the case of ideal system), leading to the formation of 4-piece chaotic attractor, converging to the robust chaotic area. The chaos is robust in the sense it is not interrupted by presence of stable periodic windows within the whole range of increasing bifurcation parameter. The MCBG allows the verification of the fact that in this case the great amount of unstable periodic orbits of *P4*, *P8*, *P16*, *P32* etc. appear at the point of the first BC (see Fig.4. point *(A)*, where only unstable branches of *P4* and *P8* are shown for the sake of simplicity). Thus the overall classical period doubling cascade is formed within the single point in the bifurcation diagram without the appearance of any stable subharmonic orbits.

All the subsequent BC do not allow the formation of any stable orbits (see e.g. points *(B)* and *(C)* in the Fig.4.).

The structure of chaotic modes of operation and the mechanisms of transition to chaos noticeably change with the introduction of even slight delay in the control circuitry of DC-DC converter.

Fig.5 shows the bifurcation diagram of boost converter for $\Delta t_d$ =0.05**T* (s). As it could be seen, the presence of delay does not affect the way the main *P1* mode of operation losses its stability – the classical period doubling bifurcation is observed. However, the following dynamics is formed by the non-smooth nature of collisions with two borderlines (see (1) and (2)), crossing the branches of bifurcation diagram.

$I_{border2}$ causes the appearance of discontinuity in the stable branch of $P2_1$ regime (see Fig. 5. point *(D)*) after which the next collision with the $I_{border1}$ (see Fig. 5. point *(E)*) changes the bifurcation sequence (in comparison to Fig.4) – the non-smooth transition to stable *P4* regime is observed. On the interval $I_{ref}$ = 0.45…0.55 (A) the transition to robust chaos is defined not by the multiple piece chaotic attractors, but by the sudden appearance and non-smooth transitions of subharmonic modes of operation caused by BC with both of the defined borders.

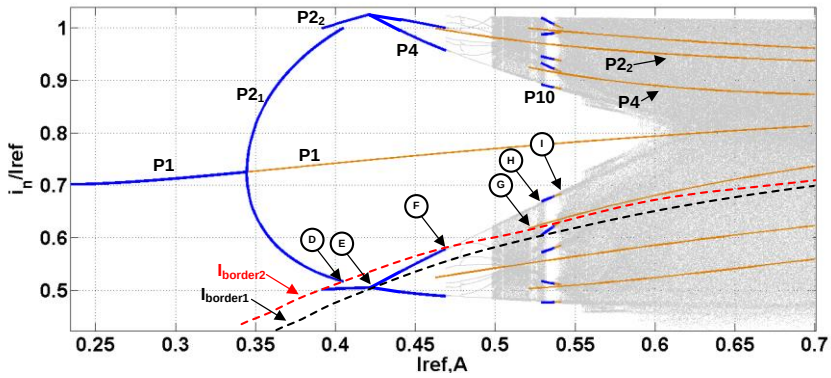


**Fig.5. The complete bifurcation diagram of the boost SPC with $\Delta t_d$=0.05**T* (s)**

One distinguishing feature of the diagram, shown in the Fig. 5, is that there is the region of coexistence of two stable *P2* regimes in the neighborhood of the first BC point (around $I_{ref}$ = 0.4 (A)). Two different types of fixed points could be detected here – one is the attracting node with both characteristic multipliers real ($P2_1$), and the other – spiral attractor with complex conjugate characteristic multipliers ($P2_2$). Each of the regimes has its own basin of attraction. However, this bistability region is not important for practicing engineers, as it exists for very narrow range of bifurcation parameter, the periodicity of coexisting regimes is the same and the coordinates of fixed points are relatively close, so

any excessive voltages or currents that could damage components of the switching power converter are not observed in this case.

As it could be seen from Fig.5, the $P2_2$ regime after the collision with $I_{border1}$ at point *(E)* does not just lose its stability, but disappears, meaning that the presence of stable or unstable period-2 regimes could not be detected to the right of the BC point with any numerical methods. However, the unstable branch of this regime is later detected in the vicinity of point *(F)*, where the *P4* regime disappears. The *P4* regime reappears at point *(G)*. The nature of the disappearance and sudden appearance of such periodic regimes in non-smooth systems up to author's knowledge is not yet clear and should be studied in details. In [10] this phenomena has been defined as "cutting border collision", as just after BC point no periodic orbit of the same periodicity is observed.

In the region between $I_{ref}$ = 0.5…0.6 (A), the appearance of *P10* window is defined by both borderlines. The collision with $I_{border1}$ leads to the non-smooth transition from chaotic mode of operation to *P10* orbit (see Fig.5 point *(H)*). However, as the value of $I_{ref}$ is further increased, the periodic window does not form classical period doubling route to chaos – the collision with $I_{border2}$ defines direct abrupt transition to chaotic mode of operation (see Fig.5 point *(I)*).

The described *P10* regime is the last periodic window within the chaotic region and all the following periodic orbits occur to be unstable, not causing the interrupts of robust chaotic operation as the bifurcation parameter is varied.

It should also be mentioned that the first relevant transition from the only practically acceptable stable *P1* operation to *P2* mode in this case appears almost at the same value as in the system without the delay$I_{ref}$≈0.36 (A). Thus, the introduction of relatively small delays do influence the dynamics of the system only after the first smooth period-doubling bifurcation.

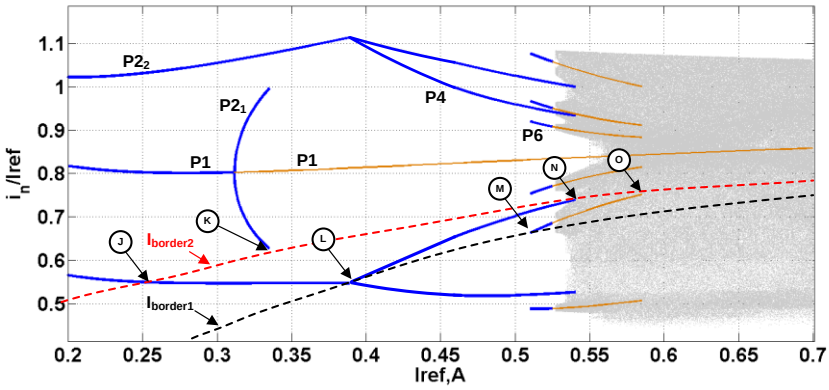


**Fig. 6. The bifurcation diagram of the boost converter with $\Delta t_d$=0.2*$T$ (s)**

The last complete bifurcation diagram (see Fig.6) depicts the case of $\Delta t_d$ = 0.2*$T$ (s), when the complete structure of the bifurcation diagram drastically changes in comparison to Fig. 5. For small values of $I_{ref}$ two coexisting regimes,

namely *P1* and $P2_2$, define the dynamics of the SPC. In this case the system could not reliably operate in the required stable *P1* mode, as even small amount of noise (always present during the operation of SPC) could lead the system to operate in $P2_2$ regime with much higher voltages and currents. At $I_{ref} \approx 0.32$ (A) the smooth transition from *P1* to $P2_1$ regime occurs. However, no period-doubling route to chaos is observed for this branch of bifurcation diagram, as the $P2_1$ branch disappears just after the collision with $I_{border2}$ (see Fig. 6 point (K)). It is interesting to note that the collision of $P2_2$ regime with the same borderline does not change the topological structure of this branch (see Fig.6 point *(J)*). The BC at point *(L)* causes disappearance of $P2_2$ regime and transition to stable *P4* mode of operation that subsequently does not lead to the formation of chaotic region through period-doubling cascade, as it "cut off" at point *(N)*.

**The subsequent chaotization of the system is governed by the appearance of *P6* orbit at point *(M)* that forms the chaotic attractor at $I_{ref} \approx 0.53$ (A) and also disappears after the collision with $I_{border2}$ (see Fig.6 point *(0)*). The subsequent chaotic region is robust, as the two borderlines do not allow the formation of stable periodic orbits or coexisting attractors.**

## 4 Conclusions

This paper showed that the discrete-time model of the boost type SPC under current-mode control could be effectively improved, including the value of total delay in the control loop. The results of complete bifurcation analysis confirm that even small values of delay may drastically change the structure of bifurcation diagrams, causing the appearance of highly non-smooth events and uncommon routes to chaos. The most distinctive phenomena include the appearance of coexisting attractors even in the region of *P1* operation, as well as sudden disappearance and reappearance of stable and unstable periodic regimes after border collisions. The obtained results prove that it is not possible to provide reliable prediction of operating modes and their stability of SPC without taking into account time lag effects. It should be noted, that relatively small values of delays (up to 20% of switching period) were chosen, considering the analog control loops. However the typical values of delays in digital control circuitry could be much greater and the effects of these delays on the global dynamics of SPC will be addressed in the future research.

## Acknowledgements

This research was funded by a grant (No. 467/2012) from the Latvian Council of Science.

## References

1. E. R. Vilamitjana, E. Alarcon, A. El Aroudi. Chaos in switching converters for power management. New York: Springer, 2012.
2. C. K. Tse, M. Li. Design-oriented bifurcation analysis of power electronics systems, *Int. Journal of Bifurcations and Chaos*, vol. 21, no. 6, pp. 1523–1537, 2011.
3. S. Banerjee, S. Parui, A. Gupta. Dynamical effects of missed switching in current mode controlled dc-dc converter, *IEEE Trans. on circuits and systems*, vol. 51, no. 12, pp. 649–655, 2004.
4. D.C. Hammil, J.H.B. Deane, D.J. Jefferies. Modeling of chaotic dc/dc converters by iterative nonlinear mappings. *IEEE Transactions on Circuits and Systems Part I*, vol.35, no.8, 25-36, 1992.
5. S. Banerjee and G. C. Verghese (Ed.) . Nonlinear Phenomena in Power Electronics. Attractors, Bifurcations, Chaos, and Nonlinear Control, IEEE Press, 2001.
6. M. Zakrzhevsky, "Bifurcation theory of nonlinear dynamics and chaos. Periodic skeletons and rare attractors", Proc. 2 nd Int. Symposium (RA 2011), pp. 26–30, 2011.
7. M.V. Zakrzhevsky and D. A. Pikulin (Eds.). Rare Attractors in Discrete Nonlinear Dynamical Systems, Riga, Latvia, 2013.
8. D. Pikulins. Complete Bifurcation Analysis of DC-DC Converters Under Current Mode Control, *Journal of Physics: Conference Series „Physics and Mathematics of Nonlinear Phenomena 2013"*, Issue 1, Vol. 482, 2014.
9. D. Pikulins. Exploring Types of Instabilities in Switching Power Converters: the Complete Bifurcation Analysis, *Electronics and Electrical Engineering*, Kaunas, Lithiuania, Technologija, -No.5, pp. 76-79, 2014.
10. D. Pikulins. The Mechanisms of Chaotization in Switching Power Converters with Compensation Ramp. *CHAOS 2014 Proceedings 7th Chaotic Modeling and Simulation International Conference* , Portugal, Lisbon, 7-10 June, 2014. pp.367-375.